Liquid Crystals
Publication details, including instructions for authors and subscription information:
http://www.informaworld.com/smpp/title~content=t713926090

Helicity of the SmC*alpha phase and its variations in a thiobenzoate series

Valerie Laux

Online publication date: 06 August 2010

To cite this Article Laux, Valerie(1999) 'Helicity of the SmC*alpha phase and its variations in a thiobenzoate series', Liquid Crystals, 26: 3, 361 — 373
To link to this Article: DOI: 10.1080/026782999205137
URL: http://dx.doi.org/10.1080/026782999205137

LIQUID CRYSTALS, 1999, VOL. 26, NO. 3, 361–373

Helicity of the SmC^*_α phase and its variations in a thiobenzoate series

VALERIE LAUX, NOEL ISAERT*, GILLES JOLY

Laboratoire de Dynamique et de Structure des Matériaux Moléculaires, URA CNRS 801, UFR de Physique Bât. P5, Université de Lille I, 59655 Villeneuve d'Ascq, France

and HUU TINH NGUYEN

Centre de Recherche Paul Pascal, CNRS, Av. A. Schweitzer, 33600 Pessac, France

(*Received 10 June 1998; in final form 27 September 1998; accepted 1 October 1998*)

We have studied by optical means a thiobenzoate series exhibiting SmC^*_A, SmC*, SmC^*_{FI} and SmC^*_α phases. We have made pitch measurements on the SmC^*_A and SmC* phases using the Grandjean–Cano method. Observing free surface drops in the SmC^*_α phase, we found periodic ellipticity fringes, due to a helical structure, and measured their optical period versus temperature; this can reach very small as well as significant values. It does not exhibit a single evolution and appears incoherent at first sight, but always follows one part of a general behaviour, depending on the thermal history of the sample. Lastly we compare experimental results with one of the structural models proposed for the SmC^*_α phase.

1. Introduction

Since the antiferroelectric liquid crystal MHPOBC was discovered, numerous chiral compounds presenting the SmC^*_A, SmC*, SmC^*_{FI} and SmC^*_α phases have been synthesized. Many studies have been made of the properties of these phases, allowing the determination of the structure for two of them: molecules of adjacent layers are tilted in the same direction in the SmC* phase, and in opposite directions in the SmC^*_A phase. Moreover both phases are helicoidal, their pitch being much bigger than the layer thickness. Concerning the ferrielectric SmC^*_{FI} phase and the SmC^*_α phase, and in spite of numerous experimental results reported in the literature, their structures have not yet been determined.

Let us now examine the case of the SmC^*_α phase. An X-ray diffraction study performed on MHPOBC showed that a tilt angle occurs in this phase [1]. Electro-optical measurements showed that the SmC^*_α phase behaves like an antiferroelectric phase at high temperature, and like a ferrielectric one at lower temperature [1]. No selective reflection occurs in this phase, and the rotatory power and birefringence are very weak; the SmC^*_α phase cannot be easily distinguished optically from the SmA phase [2, 3]. Several structural models have been proposed for this phase: optical studies hesitate between a random local dynamic helical structure, and a helical structure with a short pitch. A Devil's staircase model has also been suggested by Hiraoka and co-workers [1, 4], and a discrete phenomenological model by Zeks and Cepic [5, 6].

We have studied by optical means a series of thiobenzoate compounds exhibiting SmC^*_A, SmC*, SmC^*_γ and SmC^*_α phases. We have measured the helical pitch in the SmC^*_A and SmC* phases, and an optical period related to the helical pitch in the SmC^*_α phase.

In this paper we describe the two experimental techniques involved, present the compounds used for this study, and report our experimental results. We then discuss the period evolution in the SmC^*_α phase, and compare the information obtained on this phase with the structural model proposed by Zeks and Cepic.

2. Experimental techniques

In this study we performed pitch measurements on the SmC^*_A and SmC* phases and optical period measurements on the SmC^*_α phase. We used the Grandjean–Cano method for the SmC^*_A and SmC* phases, and the free surface drop method for the SmC^*_α phase. Both methods have already been described [7, 8]; we shall remind the reader of them briefly, as applied to our compounds. Samples were placed in a Mettler FP5 hot stage and observed using an Ortholux Leitz polarizing microscope in the reflection mode. Samples were prepared as explained for each method in the following paragraphs.

*Author for correspondence.

Journal of Liquid Crystals ISSN 0267-8292 print/ISSN 1366-5855 online
http://www.tandf.co.uk/JNLS/lct.htm
http://www.taylorandfrancis.com/JNLS/lct.htm

2.1. *Grandjean–Cano method*

The liquid crystal was introduced into a prismatic cell made of two glass slides. This cell was previously calibrated using wedge fringes, and had a very small angle ($< 0.5°$). The glass slides were rubbed unidirectionally on a velvet surface coated with diamond powder. For the smectic phases studied, this surface treatment generates a pseudo-homeotropic orientation: the helical axis is then perpendicular to the glass slides; it also fixes the projection of the directors in one single direction, near each glass surface. These conditions create a $k\pi$ twist in the cell, and generate a Grandjean–Cano step lattice. The lattice period is equal to one half the pitch in the SmC^*_A phase, and one full pitch in the SmC* phase.

For the SmC* phase many steps parallel to the cell edge can be produced, allowing precise measurements of the pitch and of its temperature dependence. For the SmC^*_A phase only a few steps are available.

It must be pointed out that the Grandjean–Cano method does not usually work over all the SmC* temperature domain: approaching the transition to the SmA phase, the tilt angle θ decreases. The rotatory power (RP) and birefringence (δn) for waves parallel to the smectic layers, depending, respectively, on θ^4 and θ^2, also decrease. The contrast of the Grandjean–Cano threads also diminishes, and threads become no longer visible. In the same temperature interval a pitch fall is also observed and measurements then become very difficult.

In one case it is however possible to perform measurements even close to the SmA transition: when the liquid crystal displays selective reflection colours. Selectively reflected wavelengths λ_{SR} range in the interval $[n_0 p, (n_0 + \delta n)p]$, where p is the helical pitch, and n_0 and $n_0 + \delta n$ are the fast and slow refractive indices, respectively. The interval is centred on $\lambda_{SR} \cong np$ (where $n \cong 1.5$ is the average refractive index).

For the SmC^*_A phase, $\lambda_{SR} \cong np$ belongs to the visible domain if $0.25\,\mu m < p < 0.5\,\mu m$. For the SmC* phase, two reflection orders are visible: the first one corresponds to $\lambda \cong 2np$ ($0.13\,\mu m < p < 0.25\,\mu m$) and the second one to $\lambda \cong np$ ($0.25\,\mu m < p < 0.5\,\mu m$).

The compounds studied display such a pitch range in the SmC* phase: the liquid crystal always exhibits selective reflection colours, and Grandjean–Cano steps are visible almost up to the high temperature transition. This allowed us to measure the pitch using the steps to within half a degree of the phase transition. When the steps were no longer visible, we obtained a good estimation of the pitch from the first order selective reflection colours.

When the rotatory power, the birefringence, or the helical pitch become very weak, as for the SmC^*_α phase and also for 'short pitch' SmC* phases ($p < 0.13\,\mu m$) [9], the Grandjean–Cano method can no longer be used. We then had to use another method, observing free surface drops.

2.2. *Free surface drops method*

The sample was a very flat drop (a few μm) deposited on a glass slide previously unidirectionally rubbed. The liquid crystal has a spontaneous pseudo-homeotropic orientation, and close to the glass surface projection of the directors follows one single direction. The directors can precess in the sample volume up to the drop surface.

Under these conditions, we observed moving Friedel fringes due to the periodic variations of the ellipticity of the light propagating in a twisted birefringent structure. This optical phenomenon is well known for N* and SmC* phases [7], and is easily observed in transmission mode. In the case of the SmC^*_α phase, it is more difficult to observe Friedel fringes, because δn becomes very weak near the SmA phase. A short theoretical calculation shows that the observation in reflection mode quadruples the contrast of the fringes [10]. We thus worked only in the reflection mode, with a quarter wave plate placed before the analyser, and the analyser uncrossed by a few degrees [8].

We also observed wedge fringes due to interference between light reflected on the liquid crystal–air and liquid crystal–glass interfaces. These fringes allowed us to calibrate the shape of the drop: one of them corresponds to a thickness variation given by $\lambda/2n$ (λ being the incident wavelength and $n = 1.5$ the average refractive index). If λ corresponds to the visible domain centre ($\approx 0.54\,\mu m$), we obtain a thickness variation of about $0.17\,\mu m$. Wedge fringes do not move when the temperature varies, showing that the drop shape does not change during experimental runs.

Comparing Friedel fringes with wedge fringes, we were then able to evaluate their optical period L. For the SmC^*_α phase and short pitch SmC* phases Friedel fringes were usually tighter than wedge fringes, and their period a fraction of $0.17\,\mu m$. Such values require a very small thickness variation of the sample, and so a very flat drop.

The optical period L depends on the helical pitch, and that depends on the temperature in the phases studied. To perform period measurements, we thus observed the evolution of Friedel fringes versus temperature: all fringes appearing in one wedge fringe for different temperature values are numbered—usually from one to about seven Friedel fringes for one wedge fringe.

The relation between L and p depends on experimental conditions and on the phase structure. In SmC*, a theoretical calculation, based on de Vries theory, shows that $p \cong 2L$ when the pitch is shorter than the Mauguin limit $2\lambda/\delta n$ and much longer than the smectic layer thickness [11]. We can thus easily obtain the pitch

evolution versus temperature. Measurements are perfectly reproducible and give a well determined curve $p = f(T)$ [9]. In SmC^*_α, the existence of a regular helix is not yet clear; the de Vries theory and the relation $p \cong 2L$ are probably not appropriate over the whole temperature domain, mainly when L is very short (a few layers). We thus preferred to plot the double optical period $(2L)$ versus temperature.

As previously explained, this method allows measurements in special experimental conditions, when the Grandjean–Cano method can no longer be used; but it presents some important difficulties. Because of the weakness of RP, δn or p, both types of fringes lose contrast and sharpness near the transition to the SmA phase. Observation and measurements are then very difficult. A good sample must have very thin areas where wedge and Friedel fringes are regular and perfectly parallel, and where the Friedel fringe evolution is not impeded by defects arising in the drop. Contrary to the prismatic cell geometry, the drop geometry cannot be checked: these conditions are not easy to obtain all together.

In SmC^*_α other difficulties can arise from the period evolution versus temperature.

(1) The optical period can sometimes change very quickly in a very short temperature range; fringes tighten (or move apart) so fast that it is impossible to perform any measurements, even if the temperature changes very slowly.
(2) At certain temperature the Friedel fringes move apart and become larger than the wedge fringes; no measurement can then be performed. The period reaches significant values on our sample scale because the fringes disappear and the sample surface becomes uniform. But since a sample exhibits a thickness variation of about 1 μm, a period greater than 1 μm could not be measured.
(3) On the sample surface the Friedel fringe period can increase at one place and decrease at another. The movements of the fringes seem to be contradictory.
(4) At first sight experiments are not reproducible, and exhibit no coherence: we observe different period evolutions for different experimental runs. Nevertheless, a careful study allows us to bring out either a general behaviour, or a few scenarios depending on initial conditions. We thus never get one well defined $L = f(T)$ curve, as for the SmC* phase, but several scenarios arise for the same compound. We shall report for each compound all the scenarios observed.

3. Experimental results

3.1. *Compounds*

The compounds studied belong to a thiobenzoate series which has already been reported [12, 8]. The general formula is:

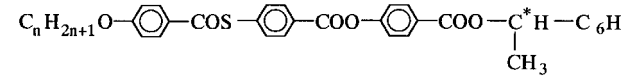

where $n = 8$ to 12. For each compound, the table displays the phase sequence and transition temperatures measured by DSC.

For $n = 10$, 11, 12, the compounds exhibit the most complete phase sequence, with six mesophases: Cr–SmC^*_A–SmC^*_{FI1}–SmC^*_{FI2}–SmC*–SmC^*_α–SmA–I. When n increases the SmC* and SmC^*_A intervals become larger, the SmC^*_{FI} and SmC^*_α intervals tighten (from 7.2°C to 4°C for the SmC^*_{FI} phase, and from 3.4°C to 0.5°C for the SmC^*_α phase).

For $n = 9$, SmC* disappears from the sequence, and SmC^*_{FI} becomes monotropic. The SmC^*_α phase reaches its largest domain of existence, that is 6.3°C. Moreover the transition temperatures are lower than for $n \geqslant 10$, and decrease by about 10°C.

For $n = 8$, the phase sequence is very short: Cr–SmC*–SmC^*_α–SmA–I and SmC* and SmC^*_α are monotropic, but rather large in range: respectively, 22.3°C and 4.2°C. Lastly, the transition temperatures are much lower than for $n = 10$, for instance the SmC^*_α–SmA transition occurs at 86°C, instead of 130°C for $n = 12$.

3.2. *SmC^*_A and SmC* phases*

For both phases, the helical pitch was measured by the Grandjean–Cano method.

3.2.1. *For $n = 11$*

For $n = 11$ and 12, the complete phase sequence is exhibited, and the same behaviour. We report results for

Table. Transition temperatures (°C) for compounds of the thiobenzoate series, obtained by DSC [12].

n	Cr		SmC^*_A		SmC^*_{FI1}		SmC^*_{FI2}		SmC*		SmC^*_α		SmA		I
8	•	86.3	—		—		—	(57)	•	(79.3)	•	(83.5)	•	159.2	•
9	•	101.3	•	(91)	•	(97)	•	109.2	—		•	115.5	•	155.4	•
10	•	109.7	•	112	•	114	•	119.2	•	120.2	•	123.6	•	152.6	•
11	•	95.5	•	101	•	104.5	•	111	•	127	•	128	•	149	•
12	•	84.2	•	111	•	112	•	115	•	129.5	•	130	•	146	•

$n = 11$ (see figure 1); the study for $n = 12$ has already been reported [12].

In SmC^*_A the pitch is about 0.4 μm and does not vary; this value is in keeping with the selective reflection colour, bright orange. Approaching the SmC^*_A–SmC^*_{FI} transition, the colour becomes red, dark red and then enters the infrared domain, showing a sudden pitch increase (see dotted lines in figure 1). In SmC* the pitch is about 0.36 μm, and is almost constant. It increases from 0.36 μm at 112°C to 0.37 μm at 124°C; in this interval the liquid crystal is yellow to yellow green.

The pitch varies only near the phase transitions. At lower temperatures near the SmC*–SmC^*_{FI} transition, the compound reflects orange, red, dark red, and infrared light, thus showing a sudden pitch increase. At higher temperatures the pitch of about 0.37 μm at 124°C falls to 0.19 μm between 124°C and 125.9°C. Two selective reflection orders are observed in this temperature interval. The second order is for a pitch between 0.4 and 0.25 μm (and at a temperature between 124°C and 125.6°C), for which $\lambda \cong np$; the compound reflects green, blue and violet light as p decreases. The first order is for the pitch ranging between 0.25 and 0.13 μm, from 125.6°C to 126.1°C, for which $\lambda \cong 2np$; the compound reflects red, orange, green, blue and violet light as p decreases. A second colour spectrum is then visible over a narrow temperature domain.

3.2.2. *For $n = 10$*

Pitch variations are displayed in figure 2; they are similar to those observed for $n = 11$, except near the SmC*–SmC^*_α transition. In SmC^*_A the pitch is about 0.5 μm, and does not vary. The liquid crystal is dark red, which confirms the measured value, and becomes colourless at the SmC^*_A–SmC^*_{FI} transition, indicating a

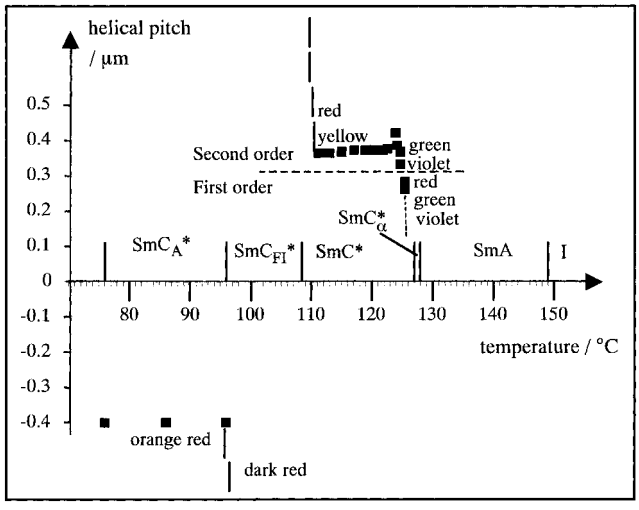

Figure 1. Helical pitch versus temperature in the SmC* and SmC^*_A phases, for $n = 11$.

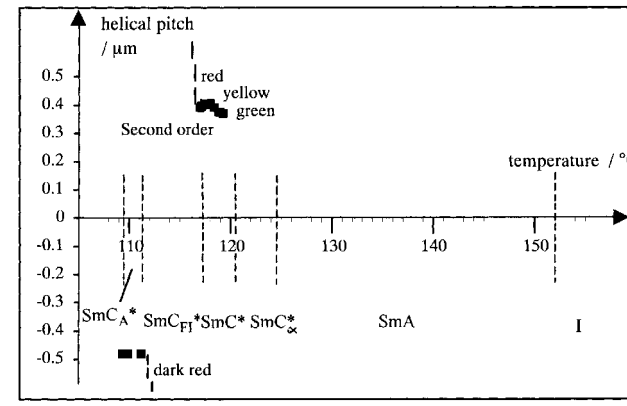

Figure 2. Helical pitch versus temperature in the SmC* and SmC^*_A phases, for $n = 10$.

sudden pitch increase. In the SmC* phase the pitch is about 0.4 μm and does not vary; the compound is orange. Near the SmC*–SmC^*_{FI} transition, as for $n = 11$, a sudden pitch increase is observed. But contrary to $n = 11$, no pitch fall occurs at higher temperatures. Only a part of the second order selective reflection is visible; the high temperature transition occurs at 119.2°C, when the compound is still green, the pitch is then about 0.37 μm.

For these three compounds ($n = 10$, 11, 12), analysis of the selectively reflected circular light shows that the double helix occurring in SmC^*_A and the SmC* helix exhibit opposite twist signs.

3.2.3. *For $n = 9$*

For $n = 9$, SmC* does not appear in the sequence. The SmC^*_A phase exhibits no Grandjean–Cano step, and is colourless in a prismatic cell. For a free surface drop, the dark red colour shows that the pitch is larger than for $n = 10$, and probably higher than 0.6 μm.

3.2.4. *For $n = 8$*

For $n = 8$, SmC^*_A does not appear in the sequence. In the SmC* phase the pitch is constant at about 1 μm. This value is bigger than for the other compounds of the series, and the phase does not give any visible reflection colour.

3.3. *SmC^*_α phase*

We shall now report optical period measurements for the SmC^*_α phase. Contrary to other helical phases, this did not show one single period evolution versus temperature, but gave several behaviours for the same compound. We were throughout able to deduce a general behaviour. The optical period evolution does not always follow it completely, but exhibits at least one part of it. This general behaviour is characterized by a weak optical period near the low temperature phase transition, a period divergence in the phase interval, and again a

weak optical period near the high temperature phase transition.

Electro-optical and conoscopic studies reported in the literature show that SmC^*_α behaves as an antiferroelectric at high temperature, becomes ferrielectric at lower temperature, and can transform into a ferroelectric SmC* phase. Transforming from an antiferroelectric phase type to a ferroelectric one, the SmC^*_α phase would change its twist sign when the temperature varies. To take these results into account, we consider that the optical period is positive at low temperature and negative at high temperature. The two temperature domains are separated by the period divergence, which is then considered as a reversal. In our report the sign change appears on the figures, but we always comment on the optical period variations in absolute values.

We shall now report the results for all the compounds studied. As mentioned above, measurements were performed using the free surface drop method. Measurements strongly depend on fringe movements and on their observations: we thus carefully describe this evolution for each experimental curve. Where fringe movements were too fast to allow precise measurement, we give only a qualitative period evolution appearing in dotted lines on the figures.

3.3.1. *For $n = 8$*

Figure 3 displays the double optical period versus temperature for $n = 8$.

On heating, at the transition fringes spread from large thicknesses and tighten very quickly towards the edge of the drop (part ○1 on figure 3); they stabilize and the interference colours are bright. The double optical period ($2L$) is about 0.07 μm at 78.1°C. When the temperature increases, this period decreases slowly to 0.05 μm at 84°C ○2 . It then increases a little at 84°C ○3 , revealing the transition to the SmA phase. The fringes do not move afterwards, and disappear gradually ○4 . Their presence in the SmA phase, which is not a helical phase, is imputed to be a memory effect.

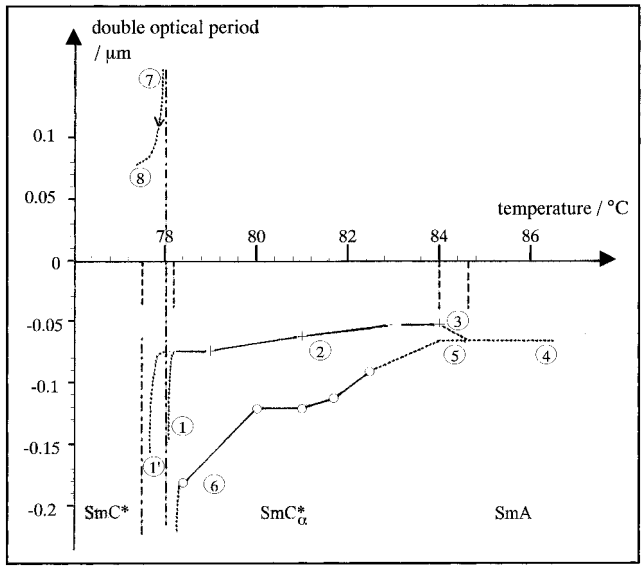

Figure 3. Double optical period versus temperature in the SmC^*_α phase, for $n = 8$, on cooling from the SmA phase (○), and on heating from the SmC* phase (+).

On cooling, the fringes are really blurred and motionless at first, and become sharp again only when the temperature reaches 84°C ○5 . The change reveals the SmA–SmC^*_α transition: from 84°C, the double optical period increases first regularly, and then more rapidly at about 78.5°C ○6 . A period divergence is then observed; the sample surface is smooth at 78°C. At 77.8°C fringes are visible again ○7 ; their double period diminishes to the transition to the SmC* phase at 77.5°C ○8 . This part of the graph is in dotted lines because no measurements could be performed.

A number of observations may be reported. (1) Some samples display a larger reversed part ○7 -○8 . (2) If heating is stopped between 81 and 84°C, the reversal observed on cooling occurs at a lower temperature; the reversed part ○7 -○8 is then narrower. (3) On cooling, if the SmC* transition is not reached after the reversal, the period behaviour is reversible on heating: it follows the path ○8 -○7 -○6 -○5 . (4) If heating is stopped before 80–81°C, no reversal is observed in the SmC^*_α phase, only a period divergence occurring at the transition to SmC*: the period then follows the path ○2 -○1′ . (5) When a sample had undergone several temperature cycles, it exhibited no reversal: the divergence occurred at the same temperature as for a fresh sample, but nothing more occurred between the divergence temperature and the SmC* transition.

For $n = 8$ the liquid crystal behaviour depends on the temperature reached in the experimental run, and on the sample age: two scenarios can be observed in SmC^*_α. The compound exhibits either the whole general behaviour, or only its high temperature part—from the period decrease occurring just after the divergence, to the weak values reached near the transition to the SmA phase.

3.3.2. *For $n = 9$*

For $n = 9$ several cycles are presented, on cooling always from the SmA phase, and on heating successively from SmC^*_{FI2}, then from SmC^*_{FI1}, and from SmC^*_A. The liquid crystal behaviour indeed depends on the phase previously reached on cooling to the lowest temperature.

On cooling, the temperature cycle always begins in the SmA phase. The period behaviour in SmC^*_α is the same whatever low temperature phase has been reached before; this is displayed in figure 4(*a*). In the SmA phase,

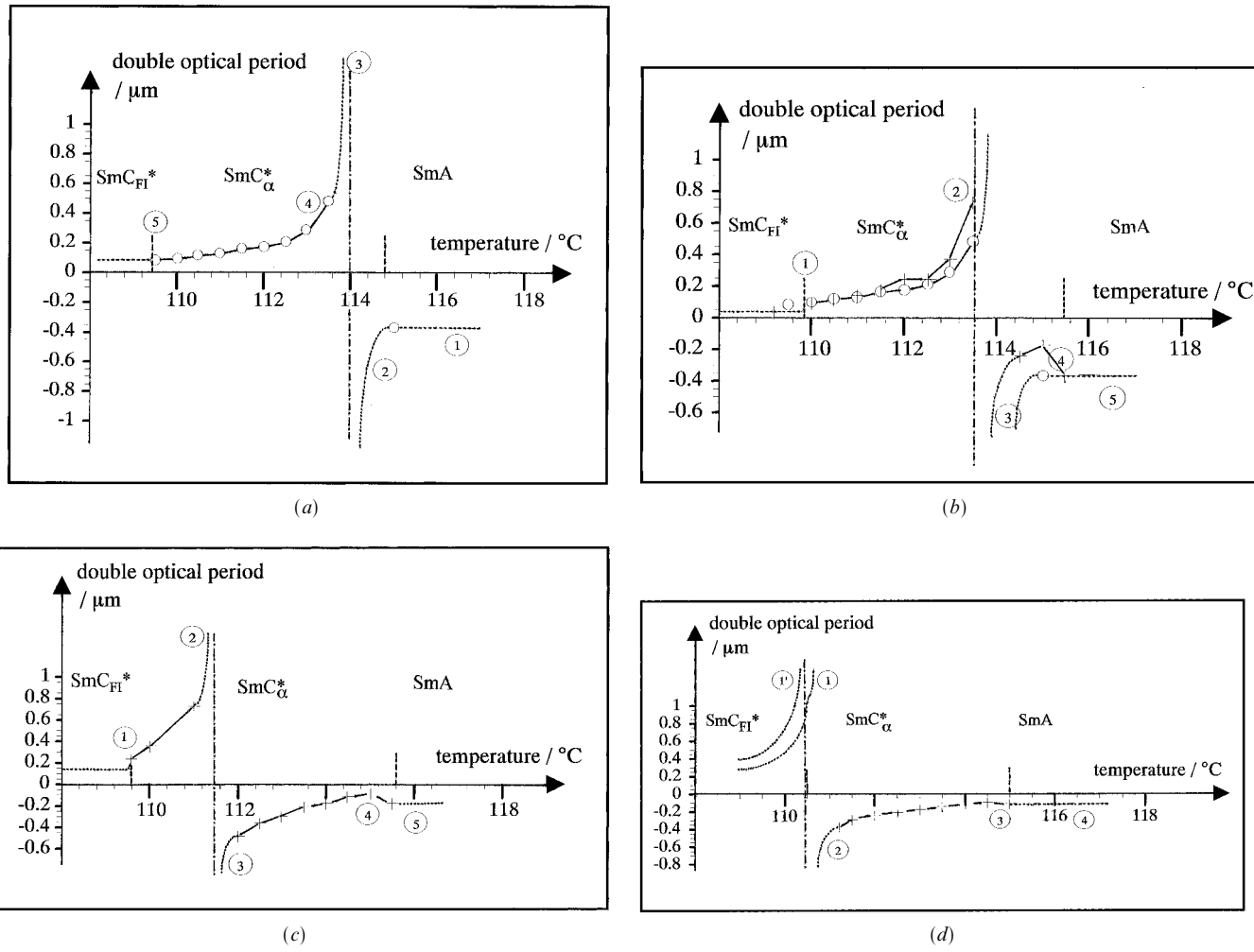

Figure 4. Double optical period versus temperature in the SmC^*_α phase, for $n = 9$, (*a*) on cooling from SmA; (*b*) on cooling (○) from SmA, and on heating (+) from SmC^*_{FI2}; (*c*) on heating from SmC^*_{FI1}; (*d*) for $n = 9$, on heating from SmC^*_A.

the fringes are motionless and blurred ○1 ; they become sharper and begin to move apart at the SmA–SmC^*_α transition at about 115°C. The double optical period increases from 115°C ○2 , diverges and reverses at 114°C ○3 , and then decreases ○4 to 0.1 µm at 110°C. The transition to SmC^*_{FI2} occurs at 109.8°C ○5 , and the fringes change into defects of which the double period is 0.04 µm. (Such defects are displayed in figure 5(*b*) for compound $n = 10$.)

Figures 4(*b–d*) display the compound's behaviour on heating; this depends on the thermal history of the sample. The lowest is at the temperature reached on cooling, and the biggest is the period in the SmC^*_{FI2} phase; this period determines the optical period behaviour in the SmC^*_α phase.

If cooling is stopped in the SmC^*_{FI2} phase, figure 4(*b*), the SmC^*_{FI2} defects are directly generated by the fringes; they freeze as soon as the transition is complete, and undergo no movement in the SmC^*_{FI2} phase interval. If the sample is heated again they remain still up to the SmC^*_{FI2}–SmC^*_α transition. SmC^*_{FI2} defects are very tightened: their double period is 0.04 µm. At 109.7°C this double period increases suddenly to 0.1 µm, the defects change into fringes, and the transition to SmC^*_α occurs ○1 . The double optical period is then about 0.1 µm; it increases sharply with temperature, diverges ○2 and reverses at 113.5°C. It then decreases ○3 to 0.18 µm at 115°C and increases to 0.36 µm at 115.6°C ○4 . From 115.6°C, the transition to SmA, the fringes freeze and change into blurred defects ○5 .

If cooling is stopped in the SmC^*_{FI1} phase, figure 4(*c*), the defects are motionless in SmC^*_{FI2}; they move apart gradually when the SmC^*_{FI1} domain is entered, at about 95°C. Their movements stop if the sample is heated again,

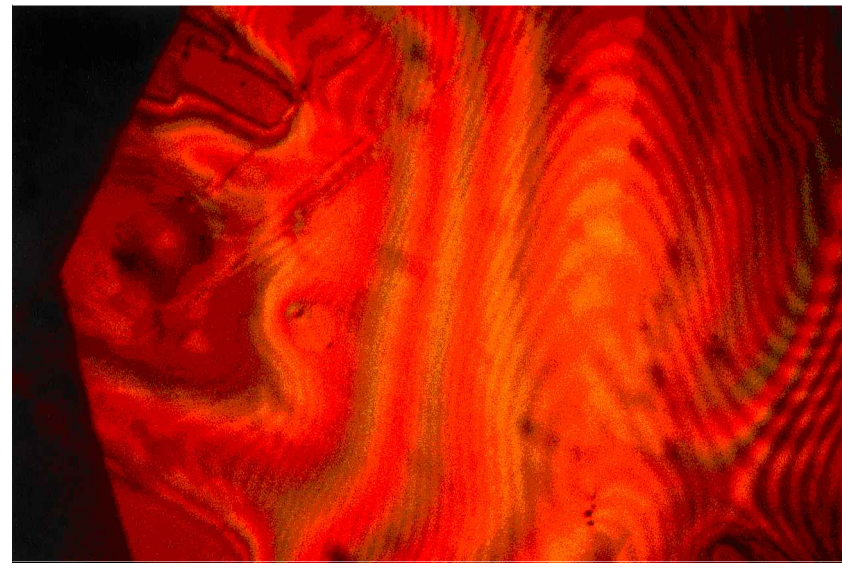

(*a*)

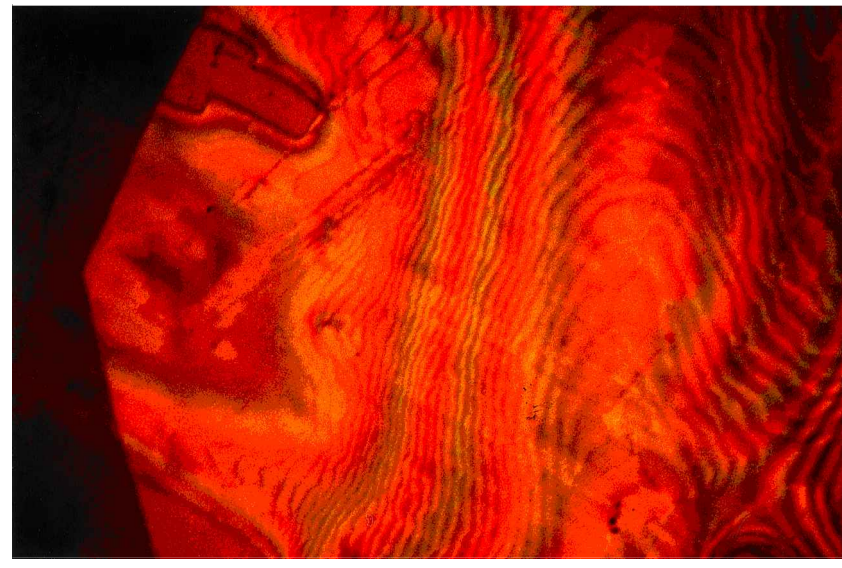

(*b*)

Figure 5. (*a*) Compound $n = 10$, at 121.4°C, on heating from the SmC* phase. This photomicrograph, taken just after the SmC*–SmC$^*_\alpha$ transition, displays a typical SmC$^*_\alpha$ texture. One can number 7 Friedel fringes for one wedge fringe, corresponding to a double optical period of about 0.05 μm (magnification ×200). (*b*) Compound $n = 10$, at 119.3°C, on cooling from SmC$^*_\alpha$; the SmC* phase has just disappeared from the sequence. A direct SmC$^*_\alpha$–SmC$^*_{FI}$ transition then occurs: Friedel fringes directly transform in SmC$^*_{FI}$ defects. These defects look like thin threads, and are very tightened close to the transition; their double period is in this case about 0.05 μm (magnification ×200).

and recur when the SmC$^*_{FI2}$ phase is reached, at 97°C. Their period continues to increase up to a double period of 0.14 μm at 108°C. At 109.7°C the period increases suddenly and the defects change into fringes: the transition to the SmC$^*_\alpha$ phase occurs. The double optical period is then about 0.24 μm [1]; it increases further with temperature and then diverges [2]. It reverses at 111.5°C, instead of 113.5°C when heating from the SmC$^*_{FI2}$ phase. It then decreases gradually [3] from 112°C to 115°C (0.5 to 0.1 μm). A slight increase [4] precedes the transition to SmA, where the fringes freeze and disappear [5].

If cooling is stopped in the SmC$^*_A$ phase, figure 4(*d*), the defects, motionless in SmC$^*_{FI2}$, move apart over the whole SmC$^*_{FI1}$ interval; they stand still again in the SmC$^*_A$ interval. When heating from SmC$^*_A$, the defects are motionless in the SmC$^*_{FI1}$ phase, and move apart again in the SmC$^*_{FI2}$ phase. At about 109°C their period is thus very large. On heating we observe either a sharp increase of the period from a large value, and the period divergence occurs just after the transition to SmC$^*_\alpha$ [1], or the period divergence occurs in SmC$^*_{FI2}$ [1′] and its reversal at the transition to the SmC$^*_\alpha$ phase. After the reversal, the double optical period decreases [2] to 0.09 μm. It increases slightly near the SmA phase [3], and at the transition to SmA at 115°C, the fringes freeze and disappear gradually [4].

As a conclusion, the thermal history of the sample has no influence on the double optical period evolution

versus temperature when cooling from the SmA phase. On the other hand, this history is very important on heating. Just after the low temperature transition, the double optical period in the SmC^*_α phase is induced by the period of the defects in SmC^*_{FI2}, or is superior to it. We observed that SmC^*_{FI1} defects move in two cases: they move apart with decreasing temperature in SmC^*_{FI1}, and with increasing temperature in SmC^*_{FI2}, if the SmC^*_{FI1} phase has been reached before. In both cases their period increases. The initial period in SmC^*_α thus depends directly on the phase reached previously on cooling. Lastly in the SmC^*_α phase, the most important point is the double optical period at low temperature, the lowest is the reversal temperature. The period value is determined by the phase reached on cooling before the heating cycle.

The liquid crystal behaviour thus depends on the thermal history of the sample, especially upon the low temperature phase reached during the experimental run. As with $n = 8$, the different scenarios can be summed up in two categories: (1) the complete general behaviour is observed, and the reversal temperature depends on sample history, (2) only the high temperature part of the general behaviour is observed.

3.3.3. *For $n = 10$*

This compound exhibits the SmC* phase in its sequence, but if the compound is open to the air, degradation seems to occur and the SmC* phase can disappear from the sequence. Several observation cycles were therefore performed. In the first stage, on heating, the cycle begins in the SmC* phase. In a second stage when the SmC* phase disappears, four different cycles are presented. They all begin in SmC^*_{FI2} on heating, but as the period of the defects increases with sample age, the double period at the SmC^*_{FI2} transition increases for each cycle.

Figures 5(*a*) and 5(*b*) show a sample for which the SmC* phase disappeared from the sequence after only one temperature cycle. The first picture (*a*) shows the texture in the SmC^*_α phase: the wedge and tightened Friedel fringes are visible. The second picture displays the SmC^*_{FI} defects, occurring at the SmC^*_α–SmC^*_{FI} transition. These defects are directly produced by the Friedel fringes, and look like thin threads; one can see that they are also very tightened.

Figures 6(*a*) and 6(*b*) display the optical period before SmC* vanishes. Two kinds of variation are observed. The first (*a*) is not new and has already been observed for $n = 9$, figures 4(*b*) and 4(*c*): the complete behaviour with a period reversal and a large hysteresis is shown. Only one noticeable difference have distinguished the present SmC*–SmC^*_α transition from the SmC^*_{FI}–SmC^*_α transition: a very rapid decrease of the period $L(T)$ very close to the transition, figure 6(*a*) ○1 ○9 .

We describe now in more detail a new kind of evolution, figure 6(*b*). On heating, at the transition to SmC^*_α, fringes form very rapidly and tighten ○1 , so revealing a sharp decrease of the double optical period. The double period reaches 0.09 μm at 120.9°C. It increases then ○2 , reaching 0.36 μm at 123.4°C. Fringes keep moving apart, so revealing a divergence, and disappear gradually. On cooling, the liquid crystal behaviour is reversible. The double optical period decreases from 0.24 μm at 122.7°C to 0.07 μm at 119.4°C, the temperature at which transition to SmC^*_{FI2} occurs. This kind of evolution, i.e. a regular increase of the period $L(T)$ with neither reversal nor hysteresis, appears as the low temperature part of the general behaviour.

The SmC* phase disappears rather quickly from the sequence. Results given in figures 6(*c–f*) concern a sample for which this disappearance occurred just after the first cooling cycle. The experiments that are reported here were performed on the same sample; the older the sample, the bigger is the period of the SmC^*_{FI2} defects, and this parameter determines the period behaviour in the SmC^*_α phase.

Figure 6(*c*) describes the run for which the double period in SmC^*_{FI2} is about 0.07 μm (1); figure 6(*d*) describes the run for which this double period is 0.12 μm. The period evolution is reversible with a regular increase of $L(t)$ ○2 without any reversal. Period values are a little bigger in the second run. Figure 6(*e*) displays the run where the double period in SmC^*_{FI} is 0.18 μm. The complete behaviour is now observed on heating and cooling with period reversal and a large hysteresis. Figure 6(*f*) describes the run where defect period is large in SmC^*_{FI}. At the transition to SmC^*_α, the period is already reversed and only one branch, the high temperature one, is obtained on heating ○1 ○2 . On cooling, a curve with two branches is found again, with a period reversal. Such behaviour has also been found for $n = 9$, figure 4(*a*), cooling and figure 4(*d*) heating.

As a conclusion for $n = 10$, the behaviour in the SmC^*_α phase seems to be influenced by the sample age. The older the sample, the bigger is the double period of the defects in the SmC^*_{FI} phase. This defects double period is equal to the double optical period in SmC^*_α measured just after the SmC^*_{FI}–SmC^*_α transition, on which depends the behaviour in the SmC^*_α phase. For a weak initial period, no reversal is observed, but only a divergence. For a middle period, a reversal is observed in the SmC^*_α interval; for a large period, the reversal occurs at the phase transition, and the double optical period measured in SmC^*_α is already reversed. As for $n = 8$ and 9, we observe either the complete general behaviour or its high temperature part. A new scenario also occurs:

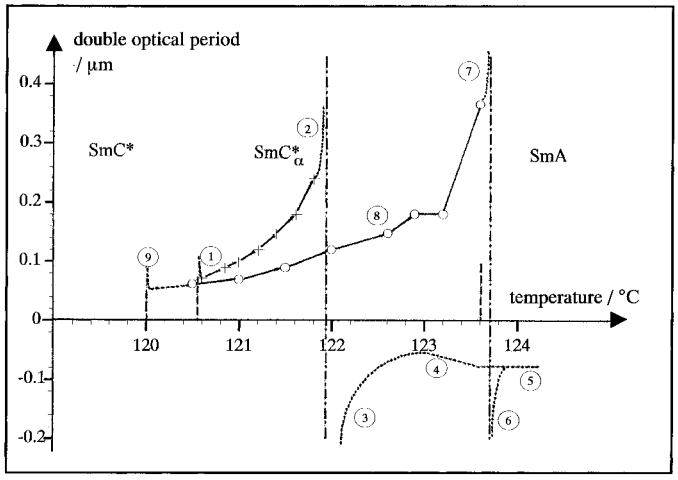

(*a*)

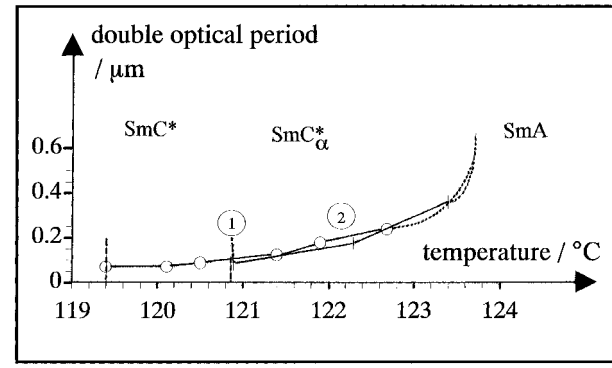

(*b*)

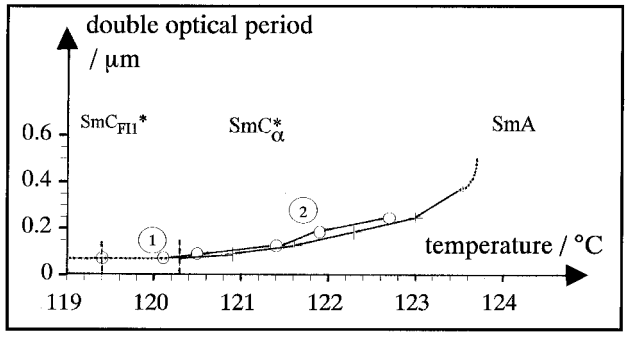

(*c*)

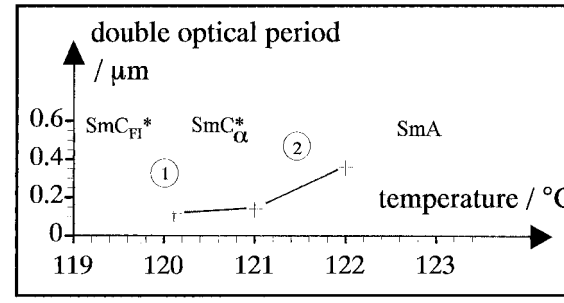

(*d*)

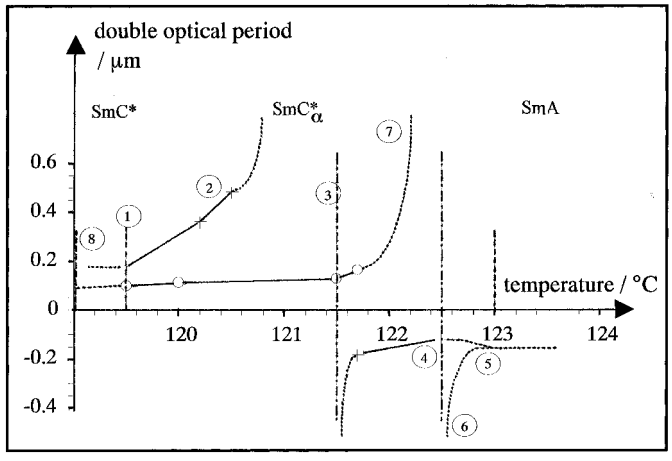

(*e*)

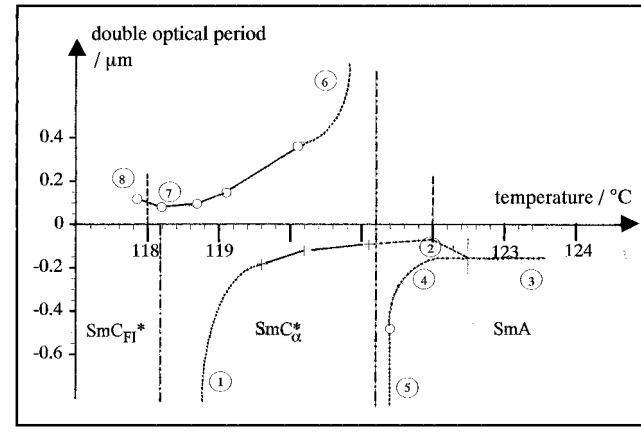

(*f*)

Figure 6. Double optical period versus temperature in the SmC_α^* phase for $n = 10$, (*a*) on heating (+) from SmC* and on cooling (○) from SmA. Parts (3)-(4)-(5), and (5)-(6) are shown in dotted lines because no measurements could be performed; (*b*) on heating (+) from SmC* and on cooling (○) from SmA; (*c*) on heating (+) from SmC_{FI}^*, and on cooling (○) from SmA. In SmC_{FI}^*, the double period is about 0.07 μm; (*d*) on heating (+) from SmC_{FI}^*, and on cooling (○) from SmA. In SmC_{FI}^* the double period is about 0.12 μm; (*e*) on heating (+) from SmC_{FI}^*, and on cooling (○) from SmA. In SmC_{FI}^* the double period is about 0.18 μm; (*f*) on heating (+) from SmC_{FI}^*, and on cooling (○) from SmA. In SmC_{FI}^* the double period is large, and diverges before the transition to SmC_α^*.

some cycles exhibit only the low temperature part of the general behaviour. In this case the optical period is initially weak; it increases and displays a divergence, without any reversal.

3.3.4 *For $n = 11$*

Figure 7 displays the optical period behaviour for $n = 11$, on heating and on cooling. For $n = 11$, the optical period evolution exhibits only the high temperature part of the general behaviour.

3.4. *Discussion*

Our study shows without doubt that a helical structure develops in the SmC^*_α phase. Besides, the optical period study gives information about the molecular organization of the sample; we have throughout to keep in mind that the study yields only average information, and not precise data on molecular positions in the bulk of the sample. Two types of information are important in our results.

First, for the optical period, we have found a general behaviour, corresponding to the most complete scenario: (1) at low temperature the optical period reaches very small values; (2) in the temperature domain of the phase it exhibits a divergence; (3) very small period values are reached again at high temperature. The double period decreases to 0.05 μm. If $p \cong 2L$, this means that only 10 smectic layers are necessary to complete a 2π rotation. Such a period has not been measured before. A structural model will have to reconcile such small values with the high values reached for the reversal; it will also have to take into account the helical structure, and to explain the period evolution.

Second, the helical structure does not seem to be well determined in the SmC^*_α phase: we cannot obtain a period evolution $L = f(T)$ that is perfectly reproducible. It depends indeed on the sample thermal history. In the general behaviour, the reversal temperature can be changed from one run to another. The general behaviour is rarely complete: we often observe only either the high temperature part or the low temperature part. Several parameters can determine the period behaviour: the temperature reached in the experimental cycle, the low temperature phase reached before heating, and the sample age. On the sample surface, different Friedel fringe lattices are visible, and they extend over very small areas. They sometimes exhibit opposite behaviours during the same experimental run.

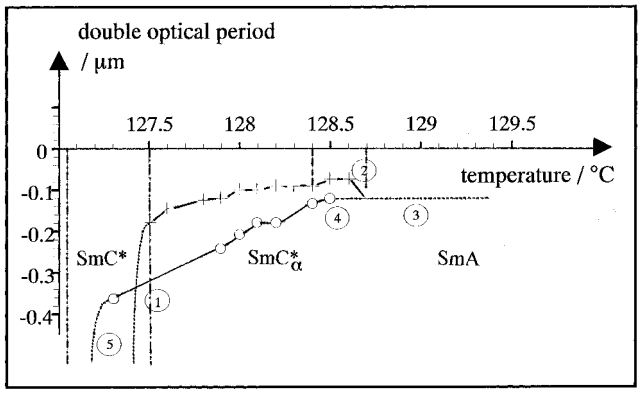

Figure 7. Double optical period versus temperature in the SmC^*_α phase for $n = 11$, on heating (+) from SmC*, and on cooling (○) from SmA.

We can deduce from these observations that the SmC^*_α phase structure is very sensitive to many external parameters, and is thus not imposed by strong molecular interactions. This information is in agreement with experimental results reported in the literature. Farhi *et al.* studied the tilt angle magnitude by Raman spectroscopy [13], and proved that this angle undergoes very important fluctuations in the SmC^*_α domain. All these characteristics are important when comparing experimental results with structural models. Any model proposed for SmC^*_α must exhibit a helical axis; besides, the molecular ordering must give the required optical period values and behaviour.

4. Confrontation with a structural model

Let us now consider a structural model that has been proposed in the literature by Zeks and Cepic for SmC^*_α. Is it in agreement with our experimental results?

Zeks and Cepic [5, 6] developed a phenomenological and discrete model, analysing the influence of the competing nearest and next nearest neighbouring layer interactions. Minimizing the free energy of the system with respect to the magnitude of the tilt angle Θ and the phase difference between two neighbouring layers α, they obtained four solutions. Three of them correspond to SmA, SmC* and SmC^*_A phases; the fourth one gives the SmC^*_α structure. The tilt angle of the molecules is constant through all the layers, the phase difference between two nearest layers α is also constant, and the helicoidal modulation extends over only a few layers. The phase difference α is rather important.

When interactions between nearest and next nearest layers change with increasing temperature, the angle α can also change, from about 0 to π. Figure 8(*a*) displays this evolution for increasing temperature, with respect to the structure described above. We obtain a ferroelectric-like phase at low temperature, and an antiferroelectric-like one at high temperature. In between, α increases and reaches $\pi/2$ at middle temperatures.

Let us now determine the helical pitch corresponding to such a structure. In our experimental conditions, light propagates along the helical axis. Observation is only

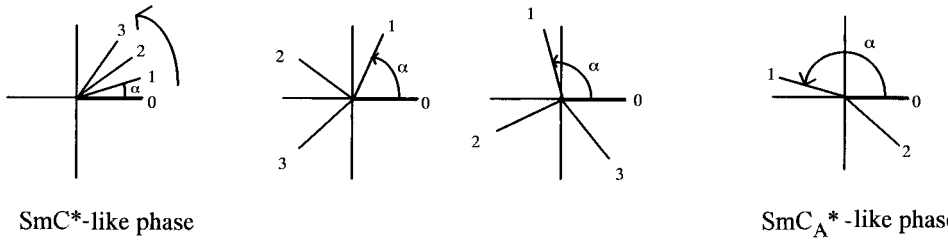

(*a*)

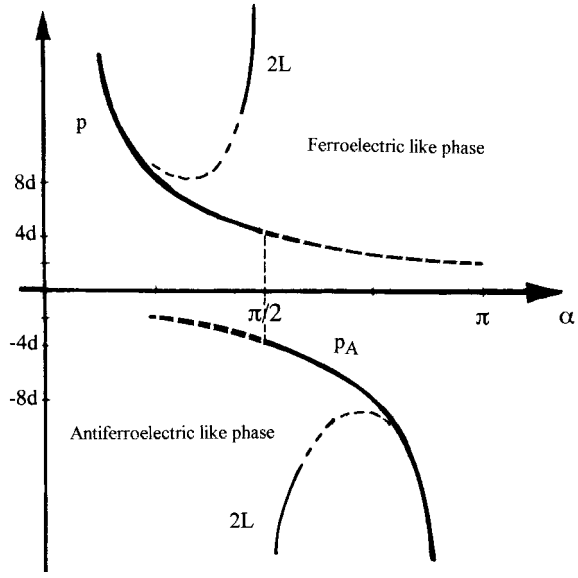

(*b*)

Figure 8. (*a*) Transformation from a SmC*-like phase to a SmC$^*_A$-like phase, when α increases. (*b*) Evolution versus α of p (pitch of a ferroelectric-like phase), p_A (pitch of an antiferroelectric-like phase), and L (optical period). When α or α' is weak $2L \cong p$. When α or α' is large $2L$ separates from p or p_A: $2L$ diverges for $\alpha \cong \pi/2$.

influenced by the optical axis projection in the plane of the layers: we are then working modulus π.

If α is weak (ferroelectric-like phase) this projection direction and the molecule projection are alike: we thus measure the real pitch $p = 2\pi d/\alpha$, where d is the layer thickness.

If $\alpha = \pi - \delta \cong \pi$ (where δ is weak, antiferroelectric-like phase) α is equivalent, modulus π, to $\alpha' = -\delta$; we thus have an apparent pitch $p_A = -2\pi d/\delta$, of opposite twist, and with a $-\delta$ phase difference between two consecutive layers. We also note that this apparent pitch p_A is the real pitch of the two helices which concern the molecular orientations of the odd and even layers of the antiferroelectric-like phase. The two domains considered have opposite twists. The twist reversal occurs for $\alpha = \pi/2$. For this value $p = 4d$ and $p_A = -4d$. Figure 8 (*b*) displays the helical pitch variations versus α.

Let us now analyse the optical period L (period of light ellipticity variations responsible for the Friedel fringes [11]) in relation to α. If α is a weak angle (ferroelectric-like phase), the twist can be considered as quasi-continuous. We are then allowed to use the de Vries theory of light propagation that leads to a double optical period nearly equal to the pitch, $p \cong 2L$. If $\alpha \cong \pi$ (antiferroelectric-like phase), $\alpha' \cong -\delta$ is weak and the de Vries theory can also be applied; the double optical period is close to the pitch p_A of the double helix: $p_A \cong 2L$. But when α or α' becomes significant, the de Vries continuous theory cannot be applied; another model of stacks of birefringent plates must be used. First developed by Reusch [14] to simulate the rotatory polarization of active crystals, this model has been applied by Joly [15, 16] to twisted mesophases. It allows the calculation of iterative vibrations that keep the same polarization states when propagating in the helical stack. Using these iterative vibrations, we are able to calculate the emergent vibration of light propagating in the sample, under our experimental conditions.

We made first a qualitative study for $\alpha = \pi/2$. In this case, for the waves propagating in the direction of the normal to the layers, we consider the directors' projection (modulus π); the structure seems no longer

chiral. The iterative vibrations are circular, and ellipticity does not vary along the stack of plates. Besides, the average refractive indices (n' and n'') have the same value for both iterative vibrations. The optical period, equal to $\lambda/(n' - n'')$, tends to infinity; therefore $2L$, which is equal to the pitch p or p_A when the angles α or α' are weak, separates from p or p_A when α or α' are larger, and diverges when $\alpha \cong \pi/2$. This divergence of $2L$ is qualitatively displayed in figure 8(*b*). The period divergence experimentally observed in the most complete scenario can thus be interpreted by azimuthal angle variations crossing $\pi/2$ in the SmC^*_α temperature domain.

In conclusion, in the complete scenario, de Vries theory allows us to determine the pitch at low and high temperatures in the SmC^*_α phase, and helical stacks of birefringent plates allow us to explain the period divergence observed in the phase temperature interval. The structural model proposed by Zeks and Cepic is then at first sight in agreement with our experimental results. We are now working on the determination of the relation between p and L over the whole temperature domain, whatever value α reaches. This calculation, longer than the qualitative study, is now in progress [17].

5. Conclusions

The twist in the SmC^*_A and SmC* phases of the thiobenzoate series studied is important: most helical pitches are lower than 0.5 μm, giving rise to selective reflection of visible light. The analysis of the circularly polarized reflected light confirms that the double helix of the SmC^*_A structure and the helix of the SmC* phase turn in opposite senses. A sudden decrease of the pitch of the SmC* phase announces the SmC*–SmC^*_α transition.

A typical texture of the SmC^*_α phase has been found: very flat drops, observed using reflected light with an analyser nearly crossed with the polarizer and preceded by a quarter wave plate, show very subtle Friedel fringes due to periodic ellipticity variations of the light after propagation on and back across the sample. The period of these fringes is very small and can reach values as low as 500 Å. This observation constitutes the first direct visual evidence of the very high twist of this phase which is thus characterized by large azimuthal rotations between adjacent smectic layers.

The behaviour of this period looks very curious and complex. For a given compound, its variation versus temperature is not unique and reproducible; nevertheless it partially or totally conforms to a scenario which, in its most complete version, has the following characteristics:

(1) A sudden decrease at the SmC*–SmC^*_α transition, leading to a very weak period is measured at low temperatures.
(2) A divergence followed by a reversal occurs at intermediate temperatures.
(3) A very weak period is again measured at higher temperatures.

Three types of behaviour can occur, depending on thermal history, initial conditions, and surface effects: the whole scenario, the low temperature part, or the high temperature part. The helical structure of the SmC^*_α phase therefore appears to be very fragile, this fragility being probably due to the small tilt angle values (this phase is close to the SmA phase) associated with large values of the azimuthal angle between adjacent layers involving weak azimuthal angular correlations.

The period of the optical Friedel fringes can be analysed in relation to a structural model proposed by Zeks and Cepic; SmC^*_α could be a helical phase which undergoes an azimuthal reorientation when the temperature varies. The azimuthal angle α between two successive layers is weak at low temperature (ferroelectric-like phase), increases crossing $\pi/2$, and finally reaches values close to π (antiferroelectric-like phase) at high temperature. Such a model is able to explain the observed variations of the period of the Friedel fringes: in the lower part of the complete scenario, α is rather weak, and the double period $2L$ probably coincides with the helical pitch of the ferroelectric-like phase; in the high temperature part, α approaches π, i.e. $\pi - \delta$ where δ is rather weak; $2L$ coincides with the pitch $2\pi d/(-\delta)$ of the antiferroelectric-like phase; in the central part α crosses $\pi/2$; the structure loses its chirality for waves parallel to the smectic layers travelling on and back across the sample. This can explain the divergence of the double optical period which differs in this situation from the structural pitch period. These explanations are up to now qualitative; further theoretical and experimental investigations are in progress to give a more quantitative description.

References

[1] Takanishi, Y., Hiraoka, K., Agrawal, V. K., Takezoe, H., Fukuda, A., and Matsushita, M., 1991, *Jpn. J. appl. Phys.*, **30,** 2023.
[2] Philip, J., Lalanne, J. R., Marcerou, J. P., and Sigaud, G., 1994, *J. Phys. II Fr.*, **4,** 2149.
[3] Philip, J., Lalanne, J. R., Marcerou, J. P., and Sigaud, G., 1995, *Phys. Rev. E*, **52,** 1846.
[4] Isozaki, T., Hiraoka, K., Takanishi, Y., Takezoe, H., Fukuda, A., Suzuki, Y., and Kawamura, I., 1992, *Liq. Cryst.*, **12,** 59.
[5] Zeks, B., and Cepic, M., 1993, *Liq. Cryst.*, **14,** 445.
[6] Cepic, M., and Zeks, B., 1995, *Mol. Cryst. liq. Cryst.*, **263,** 61.
[7] Brunet, M., and Isaert, N., 1988, *Ferroelectrics*, **84,** 25.
[8] Laux, V., Isaert, N., Nguyen, H. T., Cluzeau, P., and Destrade, C., 1996, *Ferroelectrics*, **179,** 25.
[9] Li, M. H., Laux, V., Nguyen, H. T., Sigaud, G., Barois, P., and Isaert, N., 1987, *Liq. Cryst.*, **23,** 389.

[10] LAUX, V., 1997, PhD thesis, Université de Lille I, No. 2076 (unpublished).
[11] ISAERT, N., BERTHAULT, J.-P., and BILLARD, J., 1980, *J. Opt. (Paris)*, **11,** 17.
[12] NGUYEN, H. T., ROUILLON, J. C., CLUZEAU, P., SIGAUD, G., DESTRADE, C., and ISAERT, N., 1994, *Liq. Cryst*., **17,** 571.
[13] FARHI, R., and NGUYEN, H. T., 1997, *Europhys. Lett*., **40,** 49.
[14] REUSCH, E., 1869, *Ann. phys. Chem*., **18,** 628.
[15] JOLY, G., 1984, PhD thesis, Université de Lille I, No. 608 (unpublished).
[16] JOLY, G., and ISAERT, N., 1985, *J. Opt. (Paris)*, **16,** 203.
[17] DÉTRÉ, L., private communication.